Rayleigh-Taylor instabilities in stratified fluids

Karnig O. Mikaelian
University of California, Lawrence Livermore National Laboratory, Livermore, California 94550
(Received 25 January 1982)

We study the growth of Rayleigh-Taylor instabilities at the interfaces of any number N of stratified fluids forming an arbitrary density profile. Using the linear theory, we show that there are $2(N-1)$ exponential growth rates which can be found by calculating the eigenvalues of an $(N-1)\times(N-1)$ band matrix. We illustrate analytically the case $N=3$. For general N we state and outline the proofs of two theorems: the first refers to the invariance of the spectrum of growth modes under inversion ($\rho_i \rightarrow 1/\rho_{N+1-i}$, $t_i \rightarrow t_{N+1-i}$), and the second relates the spectrum of any inversion-invariant density profile having free boundaries to the spectrum of the same profile between fixed boundaries. We compare and illustrate the results of our numerical code with the case of a continuous density profile $\rho=\rho_0 e^{\beta y}$, and, setting $N=12$, we apply our technique to solving a particular problem in designing a multishell target for inertial confinement fusion.

I. INTRODUCTION AND NOTATION

Rayleigh-Taylor instabilities[1] occur when an adverse density gradient exists as, for example, in the case of a heavy fluid supported by a lighter fluid in a gravitational field. Small amplitude perturbations at the interface grow exponentially with time $e^{\gamma\tau}$ where the growth rate γ depends on the density gradient, the wavelength λ of the initial perturbations, and on the acceleration g. For the case of two semi-infinite fluids of constant density ρ_1 and ρ_2,

$$\gamma_{\text{classical}} = \pm \left[\frac{gk(\rho_2-\rho_1)}{\rho_2+\rho_1} \right]^{1/2}, \tag{1}$$

where $k=2\pi/\lambda$. The ratio $(\rho_2-\rho_1)/(\rho_2+\rho_1)$ is referred to as the Atwood number.

The growth of Rayleigh-Taylor instabilities often leads to undesirable effects like mixing and/or shell breakup when the heavy fluid is in the form of a shell of finite thickness. One method for suppressing the growth is the use of density gradients, where the transition from the light to the heavy fluid is made in discrete steps (stratified fluid) or continuously. When the interface is given some structure in this way there appear several growth modes whose rates are complicated functions of the wave number k and of the density profile, even in the linear approximation (density perturbations $\delta\rho \ll \rho$) which we use throughout this paper, the purpose of which is to calculate those growth modes as a function of k and ρ. Only the relation $\gamma \propto \sqrt{g}$, as in Eq. (1), continues to be valid in the linear approximation. We will assume that the acceleration g is constant, that the fluids are incompressible, and we neglect viscosity, heat transfer, and surface tension.

The problem of Rayleigh-Taylor instabilities arises in numerous situations and the techniques that we develop are quite general in the sense that only the density profile need be specified. Our particular area of interest for applications, however, is laser fusion, and considerable work has been done on the hydrodynamic stability requirements of imploding capsules. Numerical simulation techniques have been used[2] to solve the fully nonlinear equations, with emphasis on the laser pulse shape. Analytical models of imploding hollow shells have been applied[3] to calculate γ, with results similar to Taylor's. Ablative mass removal has a stabilizing effect[4,5] whose size depends on the details of thermal conduction near the ablation surface. By introducing an energy spread in the driving source, one can effectively achieve the stabilizing effect of a density gradient.[6] Both of these apply, of course, to the outer shell of the capsule. For inner shells the only practical method may be the introduction of a finite density gradient by converting a heavy shell of constant density into a series of subshells gradually approaching the density of the lighter accelerating shell. The formalism described in this report was developed primarily to calculate how much reduction is achieved by this method, and in Sec. VI of this paper we apply our techniques to a particular problem in the design of a laser fusion pellet; how to minimize the fastest growth mode of a multilayered shell subject to certain constraints. We do

not address the effect of Kelvin-Helmholz instabilities because ideal designs call for zero shear velocities, and the coupling of the Rayleigh-Taylor and Kelvin-Helmholz instabilities can best be studied by numerical simulations which are now underway. A letter summarizing our approach and the symmetries discovered during the course of this work was published recently.[7]

We will solve a two-dimensional problem in slab geometry: The density $\rho=\rho(y)$ is uniform in x and z directions, being a function of only y, with the acceleration g in the $+y$ direction. Small density perturbations $\delta\rho(x,y,\tau)$ are Fourier expanded and we study normal modes described by

$$\delta\rho(x,y,\tau)=\delta\rho(y)e^{ikx+\gamma\tau} .$$

To first order in $\delta\rho$, the hydrodynamic equations can be combined to yield (see Chandrasekhar[8])

$$D(\rho DW)+\frac{gk^2}{\gamma^2}W D\rho-k^2\rho W=0 , \tag{2}$$

where the function $W(y)$ describes the velocity of the perturbed fluid in the y direction

$$v_y(x,y,\tau)=W(y)e^{ikx+\gamma\tau} .$$

D is the operator $d/(dy)$.

At an infinitesimally thin boundary between two fluids, integrating Eq. (2), we obtain the jump condition

$$\Delta(\rho DW)+\frac{gk^2}{\gamma^2}W\Delta(\rho)=0 , \tag{3}$$

where $\Delta(f)=f_+-f_-$, $f_+(f_-)$ is equal to the value of f above (below) the boundary. Note that W is continuous everywhere; in Eq. (3) it stands for the value of W at the boundary. DW need not be continuous.

The second-order differential equation (2) is linear in both ρ and W, meaning γ cannot depend on the overall scale or sign of these quantities. γ must be found by solving Eq. (2) subject to proper boundary conditions, e.g., that in a semi-infinite fluid W must vanish at distances far from the boundary, or that W must vanish at a fixed boundary. This is an eigenvalue problem for γ^2, and W is the eigenfunction.

Since there are not many density profiles $\rho(y)$ for which Eq. (2) can be solved analytically, we first solve the problem for a particular profile: stratified fluid (see Fig. 1). There are two reasons for doing this: First, one might be interested in knowing all the growth modes for a layered fluid; second, one may approximate any continuous profile by a large

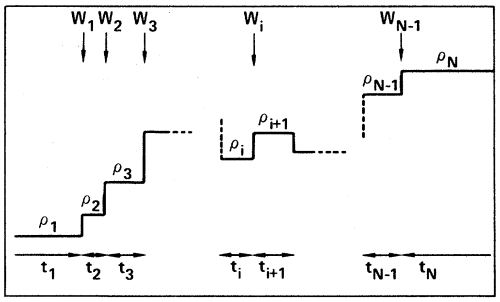

FIG. 1. General stratified density profile treated in this paper. W_i is the value of $W^{\gamma}(y)$ at interface i between ρ_i and ρ_{i+1}, $i=1,2,\ldots,N-1$, associated with the growth mode γ. There are $N-1$ possible values for γ^2.

number of thin layers whose solution will approximate that of the continuous profile—in other words, use it as a perturbation technique. We will illustrate both of these aspects.

Referring to Fig. 1, we consider N layers, each of arbitrary but constant density ρ_i, $i=1,2,\ldots,N$. ρ_1 and ρ_N are semi-infinitely thick, with the remaining layers having finite thickness t_i, $i=2,3,\ldots,N-1$. The number of interfaces is $N-1$, and we label them by $1,2,\ldots,N-1$, with 1 equal to the interface between ρ_1 and ρ_2, etc., the last interface $N-1$ being between ρ_{N-1} and ρ_N. The value of W at each interface is denoted by W_i, $i=1,\ldots,N-1$.

In each region defined by ρ_i and t_i, Eq. (2) reduces to $(D^2-k^2)W=0$, or $W\sim e^{\pm ky}$. In regions $2,\ldots,N-1$, W is a linear combination of these two solutions, while in region 1, $W\sim e^{ky}$ and in region N, $W\sim e^{-ky}$ since we require that W vanish in the $-\infty$ and $+\infty$ directions, respectively.

Of course, the $N=2$ case yields the classical result Eq. (1). In Sec. II we treat the case $N=3$ in some detail with the use of a more explicit notation. In Sec. III we consider the case of arbitrary N and show that, in general, there are $2(N-1)$ eigenvalues γ found by solving a set of $N-1$ linear homogeneous equations. We find that two different density profiles, related by "inversion", share the same spectrum of eigenvalues, leading us to the inversion theorem which states that the spectrum is invariant under $\rho_i\rightarrow 1/\rho_{N+1-i}$, $t_i\rightarrow t_{N+1-i}$.

In Sec. IV we discuss other boundary conditions which can be easily accommodated in our numerical code. We find a curious relationship between the spectra of a density profile between two fixed and two free boundaries: These two spectra are essentially identical if (and, apparently, only if) the

density profile is invariant under inversion—the fixed free theorem.

In Sec V we analytically give the eigenfunctions and eigenvalues for the case of a continuous profile $\rho=\rho_0 e^{\beta y}$ having a variety of boundary conditions, and compare the results with our multilayer approximations ($N=15$ and 20).

Finally, in Sec. VI, we apply our techniques to a particular problem in the design of a fusion target: How to spread a fixed amount of heavy material into a given number of subshells to reduce the growth of Rayleigh-Taylor instabilities. We illustrate with $N=12$. The proofs of the theorems, statements and some mathematical detail are outlined in the Appendices.

II. THE $N=3$ CASE

Consider a single layer of fluid of density ρ_2 and thickness t sandwiched between two semi-infinite fluids of densities ρ_1 and ρ_3:

region 1,

$$y\le 0,\quad \rho=\rho_1,\quad W=W(0)e^{ky};$$

region 2,

$$0<y<t,\quad \rho=\rho_2,\quad W=Ae^{ky}+Be^{-ky};$$

region 3,

$$t\le y,\quad \rho=\rho_3,\quad W=W(t)e^{-k(y-t)}.$$

Continuity of W at $y=0$ and t implies

$$\begin{aligned} A&=[W(t)-W(0)e^{-kt}]/(e^{kt}-e^{-kt}),\\ B&=[W(0)e^{kt}-W(t)]/(e^{kt}-e^{-kt}). \end{aligned} \tag{4}$$

The jump condition Eq. (3) gives

$$\frac{\gamma^2}{gk}=\frac{(\rho_2-\rho_1)}{\left[\rho_2\left[\tanh(\frac{1}{2}kt)+\dfrac{W(0)-W(t)}{W(0)\sinh(kt)}\right]+\rho_1\right]} \tag{5}$$

when applied at the first interface, and

$$\frac{\gamma^2}{gk}=\frac{(\rho_3-\rho_2)}{\left[\rho_3+\rho_2\left[\tanh(\frac{1}{2}kt)+\dfrac{W(t)-W(0)}{W(t)\sinh(kt)}\right]\right]} \tag{6}$$

when applied at the second interface. Eliminating $W(t)/W(0)$ from these last two equations we obtain a quadratic equation for $\chi\equiv\gamma^2/gk$:

$$[(\rho_3+T\rho_2)(\rho_2+S\rho_1+ST\rho_2)+\rho_2(\rho_1+T\rho_2)]\chi^2-(1+S+ST)\rho_2(\rho_3-\rho_1)\chi+S(\rho_2-\rho_1)(\rho_3-\rho_2)=0, \tag{7}$$

where $T\equiv\tanh(\frac{1}{2}kt)$ and $S\equiv\sinh(kt)$. The solutions are

$$\chi_\pm=\frac{-b\pm(b^2-4ac)^{1/2}}{2a}, \tag{8}$$

where

$$\begin{aligned} a&=(1+ST)(\rho_3+\rho_1)+S(\rho_2+\rho_1\rho_3/\rho_2),\\ b&=-(1+S+ST)(\rho_3-\rho_1),\\ c&=S(\rho_3+\rho_1)-S(\rho_2+\rho_1\rho_3/\rho_2). \end{aligned} \tag{9}$$

We have used the identity $ST^2+2T=S$ and factored out ρ_2 in deriving these expressions. The special case $\rho_2=0$ is treated below.

For arbitrary ρ_1, ρ_2, and ρ_3, one can consider two limiting cases for the wavelength λ of the perturbations: (i) Long wavelengths ($\lambda\gg t$). The two growth modes are $\chi=0$ and

$$\chi=(\rho_3-\rho_1)/(\rho_3+\rho_1),$$

independently of ρ_2. This means that long-wavelength perturbations grow at the classical rate [Eq. (1)] as if the intermediate fluid has zero thickness. (ii) Short wavelengths ($\lambda\ll t$). The two modes are

$$\chi_\pm=\frac{\rho_3-\rho_1\pm(\rho_2-\rho_3\rho_1/\rho_2)}{\rho_3+\rho_1+\rho_2+\rho_3\rho_1/\rho_2}$$

$$=\frac{\rho_2-\rho_1}{\rho_2+\rho_1}\ \text{or}\ \frac{\rho_3-\rho_2}{\rho_3+\rho_2}, \tag{10}$$

i.e., perturbations at each interface are decoupled and grow classically [Eq. (1)] with the proper Atwood numbers.

We now consider several special cases where the ratio between two densities becomes very small, very large, or equal to unity. The notation $\rho_i=0$ or $\rho_i=\infty$ is to be understood in this sense. The special cases are as follows.

(i) $\rho_1=\rho_3$. Then

$$\chi_{\pm}=\pm(\rho_1-\rho_2)/[\rho_1^2+\rho_2^2+2\rho_1\rho_2\coth(kt)]^{1/2} . \tag{11}$$

If we furthermore assume $\rho_1=\rho_3=0$, we recover Taylor's result $\chi_{\pm}=\pm 1$.

(ii) $\rho_1=0$. Then

$$\chi_+=1 , \qquad \chi_-=\frac{\rho_3-\rho_2}{\rho_3\coth(kt)+\rho_2} . \tag{12}$$

(iii) $\rho_2=0$. Then

$$\chi_{\pm}=\pm 1 . \tag{13}$$

(iv) $\rho_1=\infty$. Then

$$\chi_-=-1 , \qquad \chi_+=\frac{\rho_3-\rho_2}{\rho_2\coth(kt)+\rho_3} . \tag{14}$$

(v) $\rho_2=\infty$. This is an alternative statement of Taylor's case, viz., $\rho_1=\rho_3=0$. Therefore, $\chi_{\pm}=\pm 1$ again.

Other special cases involving ρ_3 can be obtained from the above by noticing that under $\rho_3\leftrightarrow\rho_1$, $\chi_{\pm}\rightarrow-\chi_{\mp}$. For example, $\rho_3=0$ has the growth modes $\chi_-=-1$ and

$$\chi_+=\frac{\rho_2-\rho_1}{\rho_1\coth(kt)+\rho_2} .$$

Of course, setting $\rho_2=\rho_1$ or $\rho_2=\rho_3$ takes us back to the $N=2$ case.

We observe an interesting symmetry involving ρ_2 when we go back to study the expressions for a, b, and c in Eq. (9). Since ρ_2 appears only in the combination $\rho_2+\rho_1\rho_3/\rho_2$, we conclude that both growth modes are invariant under $\rho_2\rightarrow\rho_1\rho_3/\rho_2$. For example, the two growth modes for the density profile

$$(\rho_1,\rho_2,\rho_3)=(1,10,20)$$

are identical to those of (1,2,20) for *all* wavelengths of perturbation. Notice that the operation $\rho_2\rightarrow\rho_1\rho_3/\rho_2$ interchanges the Atwood numbers at the two interfaces. An extension of this symmetry to arbitrary N will be discussed in Sec. III.

The value of ρ_2 which is invariant under the above operation, namely $\rho_2^*=\sqrt{\rho_1\rho_3}$, when the two Atwood numbers are equal, is rather special. This is the geometric mean between ρ_1 and ρ_3, and one can show that this value of ρ_2 maximizes χ_- and minimizes χ_+. The proof of this statement is outlined in Appendix A. This is true for all positive ρ_1, ρ_3, and, of course, kt. Since one is usually interested in minimizing the faster growth mode, our analysis shows that, given ρ_1 and ρ_3, the best profile has $\rho_2=\sqrt{\rho_1\rho_3}$ for any wavelength perturbations. Of course, the very long-wavelength ($\lambda\gg t$) perturbations will continue to grow at the classical rate

$$\frac{\gamma}{\sqrt{g}}=\left[\frac{k(\rho_3-\rho_1)}{\rho_3+\rho_1}\right]^{1/2} ,$$

but these are not dangerous since k is small. The short-wavelength ($\lambda\ll t$) perturbations will grow at the rate [see Eq. (10)]

$$\chi_{\pm}\underset{\lambda\ll t}{\rightarrow}(\rho_3-\rho_1)/(\sqrt{\rho_3}+\sqrt{\rho_1})^2 , \quad \rho_2=\sqrt{\rho_1\rho_3} .$$

For example, if $\rho_1=1$ and $\rho_3=10$, a single layer of $\rho_2=\sqrt{10}$ reduces the effective Atwood number from $\frac{9}{11}\approx 0.82$ to

$$9/(\sqrt{10}+1)^2\approx 0.52$$

at short wavelengths. Furthermore, this is the best one can do at any wavelength to reduce the faster growing mode.

The behavior of $\chi_{\pm}$ as a function of ρ_2 is illustrated in Fig. 2. In Fig. 3 we show the functions $W(y)$ associated with a few selected growth modes. Except for an overall factor, the functions $W(y)$ are

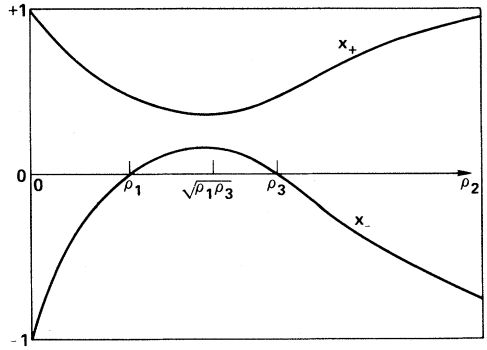

FIG. 2. General behavior of $\chi_{\pm}=\gamma_{\pm}^2/gk$ as a function of ρ_2, assuming $\rho_1<\rho_3$, for the case $N=3$. Minimum (maximum) value of χ_+ (χ_-) occurs at $\rho_2=\sqrt{\rho_1\rho_3}$. As $\rho_2\rightarrow\infty$, $\chi_{\pm}\rightarrow\pm 1$. Curves for the case $\rho_1>\rho_3$ can be obtained by using $\chi_{\pm}(\rho_1,\rho_2,\rho_3)=-\chi_{\mp}(\rho_3,\rho_2,\rho_1)$.

completely defined once we determine $W(t)/W(0)$ for a given mode with the use of Eq. (5) or Eq. (6).

From our earlier discussion we conclude that $\gamma \sim \sqrt{k}$ in both the short-and long-wavelength limits. Its behavior as a function of kt is shown in Fig. 4 for the profile $\rho=(1,\sqrt{20},20)$.

III. THE GENERAL CASE

The extension of the problem to arbitrary N is straightforward but, unfortunately, the solution is not. In this section we will write the $N-1$ equations that need to be solved for the same number of unknowns. We will show that γ^2 satisfies a characteristic polynomial equation of degree $N-1$ and therefore, in general, there are $2(N-1)$ values for γ.

Our notation was described in the Introduction and in Fig. 1. In each region i with lower (upper) boundary at $y^i_-(y^i_+)$, $t_i=y^i_+-y^i_-$,

$$W(y)=\frac{1}{\sinh(kt_i)}\{\sinh[k(y-y^i_-)]W(y^i_+)+\sinh[k(y^i_+-y)]W(y^i_-)\} . \tag{15}$$

We will use the definition $W_i=W(y^i_+)$, $i=1,\ldots,N-1$. In region 1

$$W=W_1e^{ky} , \tag{16}$$

and in region N

$$W=W_{N-1}\exp[-k(y-t_{\rm tot})] , \tag{17}$$

where we have defined our coordinate system by assuming that the first interface is at $y=0$ and defined $t_{\rm tot}$ is the total thickness of the transition region which equals $\sum_{i=2}^{N-1}t_i$.

Continuity of W implies $W(y^i_+)=W(y^{i+1}_-)$. Defining the quantity

$$\delta_i=\frac{W(y^i_-)-W(y^i_+)}{W(y^i_-)}=1-W_i/W_{i-1} , \quad i=2,\ldots,N-1 \tag{18}$$

we can write the jump conditions which extend Eqs. (5) and (6) to arbitrary N:

$$\rho_2\left[T_2+\frac{\delta_2}{S_2}\right]+\rho_1=(\rho_2-\rho_1)\frac{gk}{\gamma^2} ,$$

$$\rho_3\left[T_3+\frac{\delta_3}{S_3}\right]+\rho_2\left[T_2-\frac{\delta_2}{(1-\delta_2)S_2}\right]=(\rho_3-\rho_2)\frac{gk}{\gamma^2} ,$$

$$\vdots$$

$$\rho_{N-1}\left[T_{N-1}+\frac{\delta_{N-1}}{S_{N-1}}\right]+\rho_{N-2}\left[T_{N-2}-\frac{\delta_{N-2}}{(1-\delta_{N-2})S_{N-2}}\right]=(\rho_{N-1}-\rho_{N-2})\frac{gk}{\gamma^2} ,$$

$$\rho_N+\rho_{N-1}\left[T_{N-1}-\frac{\delta_{N-1}}{(1-\delta_{N-1})S_{N-1}}\right]=(\rho_N-\rho_{N-1})\frac{gk}{\gamma^2} , \tag{19}$$

where $T_i=\tanh(\frac{1}{2}kt_i)$ and $S_i=\sinh(kt_i)$.

Given the density profile ρ_i and t_i, and a value for $\lambda=2\pi/k$, Eq. (19) is a set of $N-1$ equations for the $N-1$ unknowns

$$\chi\equiv\gamma^2/gk,\delta_2,\delta_3,\ldots,\delta_{N-1} .$$

Eliminating the δ_i, we obtain the polynomial equation for χ,

$$a_{N-1}\chi^{N-1}+a_{N-2}\chi^{N-2}+\cdots+a_1\chi+a_0=0 , \tag{20}$$

where the coefficients are functions of ρ_i and kt_i

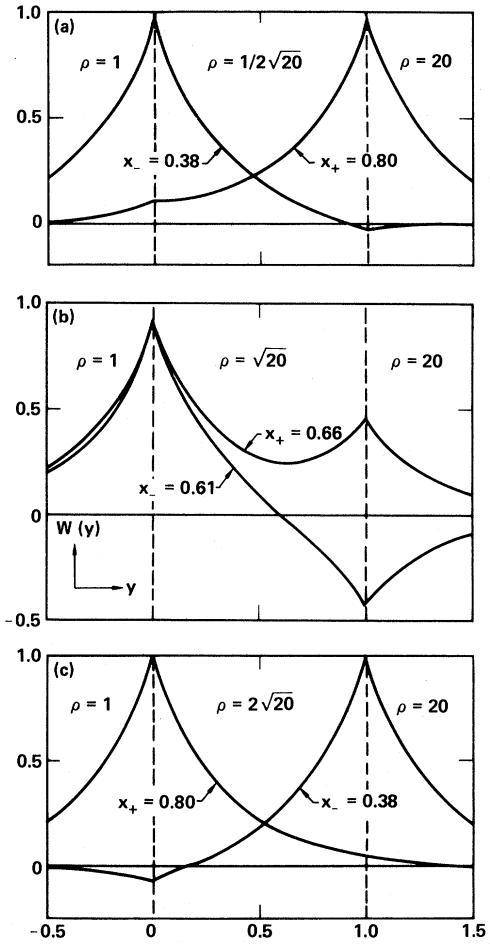

FIG. 3. Eigenfunctions $W^{\gamma}(y)$ associated with the eigenvalues $\chi_{\pm}=\gamma_{\pm}^2/gk$ for the case $N=3$. In the region $y\leq 0$ the density $\rho_1=1$ and in the region $y\geq 1$ $\rho_3=20$. We have set $t=1$ for scale, where t is the thickness of the intermediate fluid where density $\rho_2=\frac{1}{2}\sqrt{20}$, $\sqrt{20}$, and $2\sqrt{20}$ in (a), (b), and (c), respectively. The wavelength of the perturbations $\lambda=2$. We have normalized by $[W^{\gamma}(0)]^2+[W^{\gamma}(1)]^2=1$. Note that the eigenvalues are the same in (a) and (c) but the eigenfunctions are not.

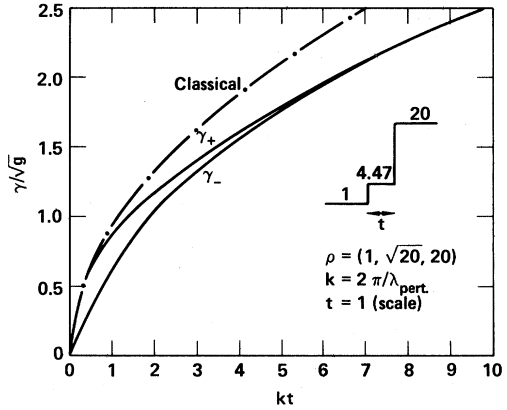

FIG. 4. Two growth rates $\gamma_{\pm}$ for the case $N=3$ with $\rho_1=1$, $\rho_2=\sqrt{20}$, $\rho_3=20$, as functions of $kt=2\pi t/\lambda$. Curve labeled Classical is $\sqrt{19k/21}$. For large values of kt the two modes become degenerate since the Atwood numbers are identical at both interfaces: $\gamma_-\rightarrow\gamma_+\rightarrow 0.8\sqrt{k}$. This is an "inversion invariant" profile. For other values of ρ_2, γ_+ and γ_- will lie above and below, respectively, the curves shown here.

only.

One can show that the roots of Eq. (20) are all real by drawing upon the work of Chandrasekhar,[8] who shows that if γ is complex then its real part is proportional to the viscosity which we neglect. Therefore, γ is either purely real or purely imaginary, and therefore, γ^2 is a real positive or negative number.

Since explicit formulas for solving polynomial equations are available only for up to fourth degree, it is clear that numerical techniques must be used for $N\geq 6$. The quartic equation for $N=5$ can be found in Appendix B.

An alternative approach makes the problem more amenable to numerical techniques, but before we describe it let us point out several features of Eq. (19). If the wavelength λ of the perturbations is much smaller than the thicknesses of the two adjacent layers, $\lambda\ll t_i, t_{i+1}$, then that interface essentially decouples from the rest and perturbations at that interface grow classically

$$\frac{\gamma}{\sqrt{g}}=\left[\frac{k(\rho_{i+1}-\rho_i)}{\rho_{i+1}+\rho_i}\right]^{1/2}.$$

If, on the other hand, λ is larger than the thickness of each region, then δ_i are all small and we can set $1-\delta_i\sim 1$ in Eqs. (19). By adding all the equations, the terms δ_i/S_i cancel on the left and $\rho_2,\ldots,\rho_{N-1}$ cancel on the right, and we obtain

$$\chi=\frac{\gamma^2}{gk}=\frac{\rho_N-\rho_1}{\rho_N+\rho_1+2\sum_{i=2}^{N-1}\rho_i T_i} \tag{21}$$

as one growth mode. Since we have assumed that $\lambda\gg t_i$, $T_i\rightarrow 0$ for all i and the above expression goes smoothly to the limit $(\rho_N-\rho_1)/(\rho_N+\rho_1)$.

Equation (21) is obtained whenever all $\delta_i\ll 1$. If several modes satisfy this condition, then the eigenvalues associated with them become degenerate and converge to (21).

Highly efficient numerical techniques are available for finding the roots of a polynomial equation like Eq. (20). The difficulty with this approach is that each of the coefficients $a_0, a_1, \ldots, a_{N-1}$ involve all of ρ_i and kt_i, although, of course, a pattern can be found for each

$$a_i = a_i(\rho_1, \ldots, \rho_N, t_2, \ldots, t_{N-1}, \lambda)$$

(see Appendix B).

Alternatively, we can write Eq. (19) in the following way:

$$\frac{1}{(\rho_2-\rho_1)}\left[\rho_2\left[T_2+\frac{1}{S_2}\right]+\rho_1\right]W_1+\frac{1}{(\rho_2-\rho_1)}\left[\frac{-\rho_2}{S_2}\right]W_2=\frac{gk}{\gamma^2}W_1\ ,$$

$$\frac{1}{(\rho_3-\rho_2)}\left[\frac{-\rho_2}{S_2}\right]W_1+\frac{1}{(\rho_3-\rho_2)}\left[\rho_3\left[T_3+\frac{1}{S_3}\right]+\rho_2\left[T_2+\frac{1}{S_2}\right]\right]W_2+\frac{1}{(\rho_3-\rho_2)}\left[\frac{-\rho_3}{S_3}\right]W_3=\frac{gk}{\gamma^2}W_2\ ,$$

$$\vdots$$

$$\frac{1}{(\rho_{N-1}-\rho_{N-2})}\left[\frac{-\rho_{N-2}}{S_{N-2}}\right]W_{N-3}+\frac{1}{(\rho_{N-1}-\rho_{N-2})}\left[\rho_{N-1}\left[T_{N-1}+\frac{1}{S_{N-1}}\right]+\rho_{N-2}\left[T_{N-2}+\frac{1}{S_{N-2}}\right]\right]W_{N-2}$$
$$+\frac{1}{(\rho_{N-1}-\rho_{N-2})}\left[\frac{-\rho_{N-1}}{S_{N-1}}\right]W_{N-1}=\frac{gk}{\gamma^2}W_{N-2}\ ,$$

$$\frac{1}{(\rho_N-\rho_{N-1})}\left[\frac{-\rho_{N-1}}{S_{N-1}}\right]W_{N-2}+\frac{1}{(\rho_N-\rho_{N-1})}\left[\rho_N+\rho_{N-1}\left[T_{N-1}+\frac{1}{S_{N-1}}\right]\right]W_{N-1}=\frac{gk}{\gamma^2}W_{N-1}\ . \tag{22}$$

The eigenvalue nature of the problem is thus obvious; the above equations can be written in matrix form

$$MW=(1/\chi)W\ , \tag{23}$$

where W is the $N-1$ dimensional eigencolumn with elements $W_1, W_2, \ldots, W_{N-1}$, $1/\chi$ is the eigenvalue, and M is a $(N-1)\times(N-1)$ band matrix whose elements can be read off from Eq. (22). Only the diagonal and the two adjacent elements of M are nonzero.

We have written a code that calculates the eigenvalues and eigenvectors of M once the density profile (ρ_i and t_i) and the wavelength λ are specified. We normalized each eigenvector by

$$\sum_{i=1}^{N-1}(W_i)^2=1\ .$$

An overall sign remains undetermined. For each eigenvalue λ the corresponding full eigenstate $W_\gamma(y)$ is calculated through the use of Eq. (15) and the computed elements of the eigencolumn W as input. Of course, the *shape* of the eigenstate $W_\gamma(y)$ does not change with time, meaning the velocity profile grows exponentially with time at the same rate at every point y, i.e.,

$$v_y(\gamma,x,y,\tau)=W_\gamma(y)e^{\gamma\tau}e^{ikx}$$

increases or decreases or oscillates (if $\gamma^2<0$) with time without changing its profile.

Applications will be discussed later. Here we explore the question of whether the symmetry found in Sec. II for the $N=3$ case can be extended to arbitrary N. We were surprised to find in our numerical calculations that indeed the spectrum, i.e., the set of γ's for a given density profile, remains the same under the following change in that profile:

$$\begin{aligned}&\rho_i\rightarrow\rho_1\rho_N/\rho_{N+1-i}\ ,\\ &t_i\rightarrow t_{N+1-i},\quad i=1,2,\ldots,N\ .\end{aligned} \tag{24}$$

Note that ρ_1 and ρ_N as well as t_1 and t_N (both infinite) do not change under the above transformation which may be called "the inversion of the profile", whereby the thickness of the lower (near ρ_1) and upper (near ρ_N) layers are interchanged, and the densities are interchanged and inverted. For example, the profile $\rho=(1,2,6,3,8)$ has the same set of four growth modes γ^2 as $\rho=(1,\frac{8}{3},\frac{4}{3},4,8)$, and this is true for *all* λ. The physical origin of this property is not clear to us. In Appendix B we outline a mathematical proof of the "inversion theorem" which reads: The spectrum associated with a densi-

ty profile is invariant under the inversion of that profile.[9]

It will prove useful to consider the Atwood number

$$r_i=(\rho_{i+1}-\rho_i)/(\rho_{i+1}+\rho_i)$$

at each interface. Since all our equations are linear in density, it is clear that an alternative way of specifying a density profile is to specify the Atwood number at each interface—e.g., one can set $\rho_1=1$ as scale, and specify $\rho_2,\rho_3,\ldots$ by specifying the Atwood numbers at the first, second,... interfaces, respectively. We can then think of the spectrum $\{\gamma^2\}$, which is a set of $N-1$ elements, as a function of another (ordered) set of $N-1$ elements $\{r_1,r_2,\ldots,r_{N-1}\}$. There is a one-to-one correspondence between these two sets if $\lambda \ll t_i$ for all $i=2,\ldots,N-1$, which we denote by the limit $\lambda\to 0$. The interfaces decouple and the perturbations grow classically:

$$\{\gamma^2\}\underset{\lambda\to 0}{\to} gk\{r_1,r_2,\ldots,r_{N-1}\}. \tag{25}$$

In general, the spectrum changes if the Atwood numbers are changed or interchanged. The one exception known to us, besides the above trivial limit, is that of inversion, Eq. (24). It is a particular permutation of Atwood numbers $r_i\to r_{N-i}$ whereby the lower and upper Atwood numbers are interchanged pairwise (if N is even, the middle Atwood number $r_{N/2}$ remains the same). Other permutations are possible, but only this particular permutation of Atwood numbers and thicknesses leaves the spectrum invariant.[10]

The inversion theorem becomes an uninteresting statement of identity when applied to a density profile which itself is invariant under inversion (since ρ does not change, the growth modes obviously do not). Such density profiles, however, have other curious properties. Let us first point out that they form a rather large class of density profiles, because requiring invariance under inversion determines less than half the profile, the rest being completely arbitrary. Examples are given later. Here we discuss two successively smaller subclasses of density profiles: The first has all equal Atwood numbers ($r_1=r_2=\cdots=r_{N-1}$) but the thicknesses matched only pairwise ($t_i=T_{N+1-i}$), and the second has all equal Atwood numbers *and* equal thicknesses.

Equal Atwood numbers imply

$$\rho_i=\rho_1\rho_N/\rho_{N+1-i}=\rho_1\left[\frac{\rho_N}{\rho_1}\right]^{(i-1)/(N-1)},\qquad i=1,2,\ldots,N$$

e.g., $\rho=(1,2,4,8,16)$. For such a profile and in the limit $\lambda\to 0$ the $N-1$ growth modes become all degenerate and converge to [see Eq. (25)]

$$\gamma^2\underset{\lambda\to 0}{\to} gkr\ , \tag{26}$$

where r is the common value of the Atwood number

$$r=\frac{(\rho_N)^{1/N-1}-(\rho_1)^{1/N-1}}{(\rho_N)^{1/N-1}+(\rho_1)^{1/N-1}}\ . \tag{27}$$

If, in addition, the thickness $t_2=t_3=\cdots=t_{N-1}$, we may take the limit $N\to\infty, t_i\to 0$. The continuous profile that is approached in this manner is easy to find, since Atwood number $\to d\rho/2\rho\to$const independent of y, and therefore $\rho=\rho_0 e^{\beta y}$. This is the one continous density profile for which Eq. (2) can be solved analytically in a rather straightforward yet nontrivial manner, as we do in Sec. V.

IV. BOUNDARY CONDITIONS

In this section we discuss how to accommodate boundary conditions other than two semi-infinite fluids of density ρ_1 and ρ_N at each end. At a fixed boundary $W=0$. For example, if the lower boundary (at $y=0$ by convention) is fixed, we delete the first of the $N-1$ equations in (22) and set $W_1=0$ in the next one. We then have $N-2$ equations and the same number of growth modes. If the upper boundary (at $y=t_{\rm tot}$) is fixed, we delete the last equation and set $W_{N-1}=0$. Thus, if both boundaries are fixed, the number of growth modes is reduced to $N-3$.

A free boundary is even easier to accommodate; simply set ρ_1 or ρ_N or both equal to zero. We have the same number $N-1$ of equations to solve and we get the same number of growth modes γ^2, although, of course, they will be different from the case of finite ρ_1 and/or ρ_N.

Two values of γ^2 are straightforward to find for the case when both boundaries are free: In Appendix B we show that any density profile having free boundaries at both ends includes $\gamma^2=+gk$ and $\gamma^2=-gk$ in its spectrum of eigenvalues. A nontrivial calculation must be carried out to find the remaining $N-3$ values of γ^2 needed to complete the spectrum. Of course, for $N=3$ these *are* the only roots as found by Taylor.

For the same density profile the eigenvalues γ and eigenfunctions $W_\gamma(y)$ are, in general, different for different boundary conditions. This is typical of boundary value problems and is particularly true in

our case, where the boundary conditions often depend explicitly on the growth modes (or vice versa); e.g., at a free boundary the condition reads

$$DW+\frac{gk^2}{\gamma^2}W=0\ .$$

We have found a curious relationship between the $N-3$ growth modes for the case of two fixed boundaries and the remaining $N-3$ nontrivial growth modes for the case of two free boundaries. These two sets become identical if the density profile is invariant under inversion. More explicitly, we have the *Fixed-Free Theorem:* Let

$$\{\gamma^2\}_{\text{fixed}} \text{ and } \{\gamma^2\}_{\text{free}}$$

be the spectrum of a density profile between two fixed and two free boundaries, respectively. If the profile is invariant under inversion, i.e., under $\rho_i \leftrightarrow 1/\rho_{N+1-i}$, $t_i \leftrightarrow t_{N+1-i}$, then

$$\{\gamma^2\}_{\text{free}}=\{\gamma^2\}_{\text{fixed}}\cup\{gk,-gk\}\ . \tag{28}$$

In our notation, the profile consists of $\rho_2,\rho_3,\ldots,\rho_{N-2},\rho_{N-1}$ layers of thickness $t_2,t_3,\ldots,t_{N-2},t_{N-1}$ between two fixed or two free boundaries. As stated earlier, the sets $\{\gamma^2\}_{\text{free}}$ and $\{\gamma^2\}_{\text{fixed}}$ contain $N-1$ and $N-3$ elements, respectively.

Let us point out that the theorem holds for the large class of density profiles invariant under inversion—it is not necessary to have all equal Atwood numbers or all equal thicknesses, but only that they be matched pairwise. An explicit example will show how general this class is.

Let $N=18$. We can choose $t_2,t_3,\ldots,t_9$ arbitrarily, but then need to set $t_{10}=t_9$, $t_{11}=t_8$, etc., until $t_{17}=t_2$. We can choose $\rho_2,\rho_3,\ldots,\rho_9$ arbitrarily, but then need to set $\rho_{10}=c/\rho_9$, $\rho_{11}=c/\rho_8$, etc., until $\rho_{17}=c/\rho_2$, where c is again arbitrary and hence can be used to choose another density. In all, 9 out of 16 densities and 8 out of 16 thicknesses can be chosen arbitrarily.

If $N=17$, we can still choose 8 out of the 15 thicknesses arbitrarily (e.g., $t_2,t_3,\ldots,t_9,t_{10}=t_8$, $t_{11}=t_7,\ldots,t_{16}=t_2$) and choose 8 out of the 15 densities arbitrarily [e.g., $\rho_2,\rho_3,\ldots,\rho_9,\rho_{10}=c/\rho_8$, $\rho_{11}=c/\rho_7,\ldots,\rho_{16}=c/\rho_2$, but $c=(\rho_9)^2$ now].

Again, we cannot offer a physical understanding of this theorem and outline a proof in Appendix B. It follows also from a corollary to the inversion theorem applied to free boundaries ($\rho=0$) which go over to fixed boundaries ($\rho=\infty$) under inversion. Let us mention that[10] both the inversion and fixed-free theorems are statements about the eigenvalues γ and not about the eigenstates $W_\gamma(y)$. We now turn to some applications.

V. COMPARISON WITH A CONTINUOUS DENSITY PROFILE

As mentioned in the Introduction, one application of our approach is the calculation of the growth modes for a continuous density profile which cannot be solved analytically, by approximating that profile with a (large) number of density steps which we can solve numerically by the technique described in the previous sections. As another application, suppose that a desired continuous profile cannot be fabricated but that a number of layers following that profile can be coated, then one would like to know how close one can come to suppressing the growth of Rayleigh-Taylor instabilities.

In this section, we compare the multilayer approximation to a continuous profile that can be solved analytically: the exponential profile. In other cases, one would study the spectrum as a function of N.

Let us first present the analytical solutions to the density profile

$$\rho(y)=\rho_0 e^{\beta y}\ ,\quad 0\le y\le t \tag{29}$$

with various boundary conditions as shown in Fig. 5. Our notation follows Ref. 8, where case (a) is treated (fixed boundaries at both ends). The following applies to all the cases. Substituting Eq. (29) in Eq. (2), we get

$$D^2W+\beta DW-k^2\left[1-\frac{g\beta}{\gamma^2}\right]W=0 \tag{30}$$

whose general solution is

$$W=A_1e^{q_1y}+A_2e^{q_2y}\ , \tag{31}$$

where

$$\begin{aligned} &q_1+q_2=-\beta\ , \\ &q_1-q_2=\left[\beta^2+4k^2\left[1-\frac{g\beta}{\gamma^2}\right]\right]^{1/2}\ . \end{aligned} \tag{32}$$

There are two unknowns in the problem, the ratio A_2/A_1 and q_1-q_2. These are determined by the boundary conditions at the two ends. In all of the cases, the growth mode(s) γ^2 will be given by

$$\frac{\gamma^2}{g}=\frac{2ed\,k}{x^2+e^2+d^2}\ , \tag{33}$$

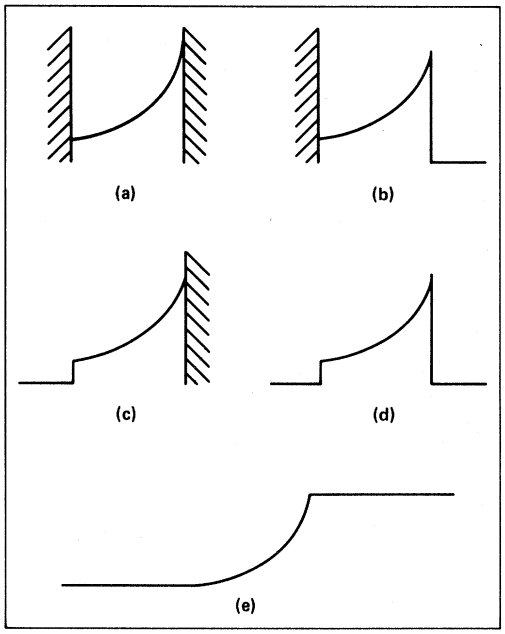

FIG. 5. A continuous exponential profile $\rho=\rho_0 e^{\beta y}$ between (a) two fixed boundaries; (b) fixed at $y=0$, free at $y=t$; (c) free at $y=0$, fixed at $y=t$; (d) two free boundaries; (e) two semi-infinite fluids of density ρ_0 for $y\leq 0$ and ρ_t for $y\geq t$.

where $e=kt$ and $d=\beta t/2$, and

$$x=\pm i(q_1-q_2)t/2$$

is to be determined in each case. All the following W's below can be multiplied by an arbitrary constant.

Case (a). Fixed boundaries at $y=0$ and at $y=t$. Requring W to vanish at $y=0$ and at $y=t$ one finds[8]

$$W=e^{-\beta y/2}\sin(m\pi y/t)\ ,\quad m=1,2,\ldots \tag{34}$$

and therefore

$$x=m\pi\ . \tag{35}$$

Case (b). Fixed boundary at $y=0$; free boundary at $y=t$. Requiring $W=0$ at $y=0$,

$$W=e^{-\beta y/2}\sin(xy/t)\ . \tag{36}$$

The condition of a free boundary is given by Eq. (3) with $\rho_+=0$. We now have

$$DW+\frac{k^2g}{\gamma^2}W=0\ . \tag{37}$$

Applying this condition at $y=t$, we get

$$\tan(x)=\frac{-2xd}{x^2+e^2-d^2}\ . \tag{38}$$

In looking for the solutions x of this transcendental equation, one must consider both real and imaginary values of x. Some care is required in solving Eq. (38) since the right-hand side can have a pole at $x^2=d^2-e^2$.

Case (c). Free boundary at $y=0$; fixed boundary at $y=t$. Requiring $W=0$ at $y=t$,

$$W=e^{-\beta y/2}\sin(x-xy/t)\ , \tag{39}$$

while condition (37) applied at $y=0$ gives

$$\tan(x)=\frac{2xd}{x^2+e^2-d^2}\ . \tag{40}$$

The same comments following Eq. (38) apply here also.

Case (d). Free boundaries at $y=0$ and at $y=t$. The free boundary condition Eq. (37) applied at $y=0$ reads

$$A_1q_1+A_2q_2+\frac{k^2g}{\gamma^2}(A_1+A_2)=0 \tag{41}$$

and, applied at $y=t$,

$$A_1q_1e^{q_1t}+A_2q_2e^{q_2t}+\frac{k^2g}{\gamma^2}(A_1e^{q_1t}+A_2e^{q_2t})=0\ . \tag{42}$$

These two equations determine the ratio A_1/A_2 and q_1 or q_2 ($q_1+q_2=-\beta$). Clearly, $A_1=A_2=0$ unless the determinant of the 2×2 matrix M vanishes, where

$$M=\begin{bmatrix} q_1+\dfrac{k^2g}{\gamma^2} & q_2+\dfrac{k^2g}{\gamma^2} \\ e^{q_1t}\left[q_1+\dfrac{k^2g}{\gamma^2}\right] & e^{q_2t}\left[q_2+\dfrac{k^2g}{\gamma^2}\right] \end{bmatrix}. \tag{43}$$

The condition $\det|M|=0$ reads

$$(e^{q_2t}-e^{q_1t})\left[q_1+\frac{k^2g}{\gamma^2}\right]\left[q_2+\frac{k^2g}{\gamma^2}\right]=0 \tag{44}$$

and the solutions are

$$W=e^{\pm ky}\ ,\quad \frac{\gamma^2}{gk}=\mp 1 \tag{45}$$

and

$$W=e^{-\beta y/2}\left[\cos(xy/t)-\frac{1}{2xd}(x^2+e^2-d^2)\sin(xy/t)\right] \tag{46}$$

with $x=m\pi$ and $m=1,2,\ldots$. It will be noted that the spectrum is identical to the case of two fixed boundaries, plus the two modes in Eq. (45), which correspond to W's peaked around $y=0(\gamma^2/gk=+1)$ and $y=t(\gamma^2/gk=-1)$. This is an example of the fixed-free theorem stated in Sec. IV.

Case (e). $\rho=\rho_0$ *for* $y\le 0$ *and* $\rho=\rho_t$ *for* $y\ge t$. In the region $y\le 0$, $W(y)=W_0e^{ky}$; in the region $y\ge t$, $W(y)=W_te^{k(t-y)}$. The continuity condition at $y=0$ reads

$$W_0=A_1+A_2 \tag{47}$$

and at $y=t$,

$$W_t=A_1e^{q_1t}+A_2e^{q_2t}\,. \tag{48}$$

The jump conditions at $y=0$ and t simplify if we choose ρ to be continuous, though the problem can be solved for arbitrary discontinuities in ρ at these two boundaries, and the solution will be presented elsewhere. For a "weak" discontinuity, i.e., ρ continuous but $D\rho$ not continuous, as shown in Fig. 5(e), Eq. (3) implies that DW is continuous. Therefore, at $y=0$,

$$kW_0=q_1A_1+q_2A_2 \tag{49}$$

and at $y=t$,

$$-kW_t=q_1A_1e^{q_1t}+q_2A_2e^{q_2t}\,. \tag{50}$$

The four equations (47)–(50) for the four unknowns W_0, A_1, A_2, and W_t, will have a nontrivial solution if and only if

$$\det\begin{vmatrix} 1 & 1 & 1 & 0 \\ k & q_1 & q_2 & 0 \\ 0 & e^{q_1t} & e^{q_2t} & 1 \\ 0 & q_1e^{q_1t} & q_2e^{q_2t} & -k \end{vmatrix}=0 \tag{51}$$

which is the characteristic equation for finding the growth modes γ. The solution to (51) is

$$\tan(x)=\frac{2xe}{x^2+d^2-e^2}\,, \tag{52}$$

another transcendental equation whose solutions x give the growth modes γ when substituted in Eq. (33) as before. The associated eigenfunctions are

$$W=e^{-\beta y/2}\left[\cos(xy/t)+\frac{1}{x}(e+d)\sin(xy/t)\right]\,. \tag{53}$$

If we consider a continuous density profile as the $N\to\infty$ limit of some stratified profile, then we expect infinitely many growth modes, since we have seen in Secs. III and IV that the number of modes γ^2 is equal to N for large N. This indeed is true for the cases considered in this section; there are infinitely many solutions x and, therefore, γ^2. A few of the solutions may come from imaginary values of x; the remaining infinity of solutions come from real values of x. In practice, one is usually interested in the largest values of γ^2, perhaps the first two or three fastest growing modes.

In general, the transcendental equations obtained in cases (b), (c), and (e) must be solved numerically. We illustrate case (e) in Appendix C. In Table I we

TABLE I. Growth rates $\gamma/\sqrt{g}$ of the first two fastest growing modes and the one stable mode for an exponential density profile between a fixed boundary and a free boundary: case (b), Fig. 5(b). The thickness t of the fluid is set equal to one for scale, and the ratio $\rho(1)/\rho(0)=20/1$, i.e., $\beta\simeq 3$. The continuous case is compared with $N=15$ and 20 stepwise simulations of the profile. Shorter-wavelength perturbations require larger values of N. In the first column $k=2\pi/\lambda$. In the very short-wavelength limit $\lambda\ll t$ the unstable modes approach $\gamma/\sqrt{g}\to\sqrt{\beta}$ while the one (unique) stable mode approaches $\gamma/\sqrt{g}\to i\sqrt{k}$.

	$\gamma/\sqrt{g}$ for case (b) shown in Fig. 5(b)		
kt	Continuous	$N=15$	$N=20$
0.5	0.36,0.14,0.59i	0.35,0.14,0.59i	0.35,0.14,0.59i
1	0.64,0.29,0.96i	0.63,0.28,0.96i	0.63,0.28,0.96i
4	1.36,0.95,2.00i	1.34,0.94,2.00i	1.35,0.94,2.00i
8	1.60,1.36,2.83i	1.59,1.37,2.83i	1.59,1.36,2.83i
10	1.64,1.46,3.16i	1.65,1.48,3.16i	1.64,1.47,3.16i
15	1.69,1.59,3.87i	1.75,1.66,3.87i	1.71,1.62,3.87i
20	1.71,1.65,4.47i	1.83,1.78,4.47i	1.77,1.71,4.47i
30	1.72,1.69,5.48i	2.00,1.98,5.48i	1.88,1.85,5.48i

compare the first three largest growth modes for the continuous profile with the $N=15$ and 20 modeling of that profile for case (b). In Table II we do the same for case (e). We have also compared the eigenfunctions $W_\gamma(y)$ and find good agreement.

At this point it becomes clear that what we are describing is a perturbation technique in which the variable is N, the exact results for the case of a continuous ρ being given by the limit $N\to\infty$. The boundary conditions, nontrivial because they contain explicitly the eigenvalues we are trying to determine, are treated exactly. Only the intermediate density profile is approximated by a series of steps and clearly the larger the number of steps the better is the modeling of that profile. The convergence properties of this technique is a whole problem in itself which we hope to treat in another paper.

Our original motivation was to find the growth modes for a discrete set of density steps like Fig. 1 which, of course, our technique solves exactly. The question arose in the context of the design of multishell targets for inertial confinement fusion (ICF). In Sec. VI we describe an application to such a design problem.

VI. AN APPLICATION TO ICF MULTISHELL-TARGET DESIGN WITH $N=12$

Rayleigh-Taylor instabilities grow in imploding ICF targets when a heavy fluid is accelerated by a lighter fluid. All designs suffer from such an instability at some time or another during the history of implosion. As mentioned in the Introduction, the outer ablating surface may be stabilized, i.e., γ (with ablation) $<\gamma_{\text{classical}}$, by conduction effects or "fire polishing." Our interest is in the inner shell(s), where this mechanism is not available, and where some degree of stability might be achieved by introducing a finite density gradient. Hence, we consider the following general, and no doubt very idealized problem: A shell of heavy fluid (e.g., Au) of thickness t_H and density ρ_H accelerated by a shell of light fluid (e.g., CH) of thickness t_L and ρ_L. Assume that the lower boundary of ρ_L and the upper boundary of ρ_H are free At their common interface, fluid instabilities will grow almost at the classical rate

$$\frac{\gamma^2}{g}=k(\rho_H-\rho_L)/(\rho_H+\rho_L) \tag{54}$$

which is large because the Atwood number is large. We say "almost" because the exact values are obtained by solving the $N=4$ problem in our notation:

$$\rho_1=0,\ \rho_2=\rho_L,\ \rho_3=\rho_H,\ \rho_4=0\ .$$

Two of the growth modes are $\gamma^2=gk$ and $\gamma^2=-gk$ peaked around $y=-t_L$ and $y=t_H$, respectively, in a coordinate system where the interface is located at $y=0$. The third mode is approximately given by Eq. (54) if $\lambda\lesssim t_L$ and $\lambda\lesssim t_H$. Its exact value will be computed below.

To reduce this growth mode (nothing can be done about the other two as long as the boundaries are free) we may insert "transitional" layers at the interface to make the transition from $\rho_L\approx 1$ to $\rho_H\approx 20$ smoother, or we may vary the density continuously at the interface. Here, we treat the case of eight transitional layers, hence we need to solve the $N=12$ problem.

One important constraint is that we do not increase the mass of the heavy fluid being accelerated, hence we speak of spreading the mass of the heavy shell into a number of subshells. Another constraint is that we have some of the heavy material still left in the last ($N=11$) shell; otherwise the problem would be trivial.

Of course, in practice, perturbations come in all wavelengths and we need some criterion as to what λ we should be worried about. This criterion comes from outside the linear regime that we have assumed throughout this paper: Perturbations grow exponentially with time until their amplitude becomes of the order of λ, after which nonlinear effects slow down the growth. Since we are interested primarily in the integrity of the last shell, and, in particular, that it does not break up, we require the amplitude of the perturbations to grow to no more than the dimensions of the last shell. This, in turn,

TABLE II. Same as Table I for Case (e), Fig. 5(e). There are no stable modes in this case.

	$\gamma/\sqrt{g}$ for case (e) shown in Fig. 5(e)		
kt	Continuous	$N=15$	$N=20$
0.5	0.66,0.23	0.65,0.24	0.66,0.24
1	0.90,0.43	0.90,0.44	0.90,0.44
4	1.46,1.11	1.43,1.12	1.44,1.12
8	1.63,1.44	1.60,1.44	1.60,1.44
10	1.66,1.52	1.64,1.53	1.64,1.52
15	1.69,1.62	1.72,1.66	1.70,1.63
20	1.71,1.66	1.80,1.76	1.75,1.71
30	1.72,1.70	1.97,1.95	1.85,1.83

implies that we should look out for wavelengths of the order of the thickness of the last shell. As more and more of the heavy material is spread into subshells, the thickness of the remaining shell is reduced and, consequently, the wavelength λ of the most dangerous perturbations. In general, as the classical expression for γ^2 illustrates, shorter wavelength perturbations grow faster. This implies that there is a limit as to how much of the original shell should be spread, since spreading more of that material might shift λ to such low values that perturbations will grow even faster. The question then is, how much of the original material can be spread before this situation is reached, and how much reduction in γ can be achieved in this way?

Let us illustrate with the following density profile: $\rho=(0,1,1.5,2,3,4,5,7,10,14,20,0)$. This is close to the profile where all the Atwood numbers are the same, which has the property that all fluid interfaces are equally unstable to very short-wavelength perturbations [see Eqs. (25)–(27)]. There are too many variables to try and determine analytically the best possible profile $(\rho_2,\rho_3,\ldots,\rho_{11})$, $(t_2,t_3,\ldots,t_{11})$, and the reasons for our choice will be discussed elsewhere. We also chose all our subshells to have equal thicknesses, so that the actual profile used is close to being invariant under inversion.

There are 11 growth rates γ^2, two of which are $\pm gk$. In Fig. 6 we plot the largest of the remaining nine modes as a function of the percentage of the mass of heavy material spread into the eight subshells. We have set λ equal to the thickness of the remaining last shell of density $\rho_H=20$. To completely specify our units, we need only mention that the thickness of the original heavy shell was used for scale $t_H(\text{original})=1$. The thickness t_2 was chosen large (specifically $t_2=6$). The percentage of the mass spread determines t_{11}, the thickness of the remaining last heavy shell; e.g., if 40% is spread, then $t_{11}=0.6$. The thickness t_{subshell} of each subshell is determined by "mass conservation," i.e.,

$$\rho_H=\sum_{i=3}^{11}\rho_i t_i=t_{\text{subshell}}\sum_{i=3}^{10}\rho_i+t_{11}\rho_H\ . \tag{55}$$

From Fig. 6 we see that the exact values of the growth modes for the original configuration (0% mass spread) are given by the classical expression, Eq. (54), to a very good approximation as claimed earlier in this section. From the same figure we conclude that the optimum design would spread only about 40% of the original material, reducing γ by a factor of 1.54.

The existence of a minimum in Fig. 6 could have been predicted on the basis of the arguments given above: Spreading too little would not change γ very much from the classical result, but spreading too much would make the design vulnerable to very short wavelengths since the last shell gets thinner, and these short-wavelength perturbations grow faster. In fact, if more than 60–70% is spread, then the nine nontrivial growth modes are given approximately by $\gamma^2=gkr_i$, where the Atwood numbers range between 0.1 and 0.2. If all the Atwood numbers were the same, it would be 0.165, and the reduction in γ would be a factor of 1.57.

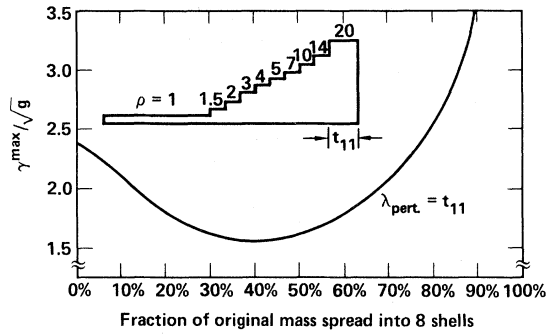

FIG. 6. Largest of the nine nontrivial growth rates for the profile shown as a function of the fraction of mass spread from the heavy ($\rho=20$) fluid into the eight transitional layers. Thickness of the original heavy fluid is set equal to 1 for scale, and the wavelengths $\lambda_{\text{pert}}=t_{11}=(1-\text{fraction spread})=\text{thickness of remaining heavy fluid}$ (the subscript pert represents perturbations).

Of course, increasing N, i.e., putting more subshells, would suppress the instability even more. Our calculations indicate that the ultimate reduction in γ is about 2.5. We must recall that the analysis presented in this paper is applicable only in the linear regime, and that fully nonlinear numerical simulations are necessary for a realistic assessment of the advantages of finite density gradients.

ACKNOWLEDGMENTS

This research was carried out as a result of a question posed by John Lindl. I am grateful to him for sharing with me his interest and insight into this problem. I would also like to acknowledge stimulating conversation with Dave Munro. This work was supported by the U. S. Department of Energy under Contract No. W-7405-ENG-48.

APPENDIX A

We will show that for the case $N=3$, i.e, $\rho=(\rho_1,\rho_2,\rho_3)$, the value $\rho_2^*=\sqrt{\rho_1\rho_3}$ minimizes the

faster growth mode χ_+ and maximizes the slower growth mode χ_- for all values of λ. Note that

$$\frac{\partial\chi_\pm}{\partial\rho_2}=\frac{\partial\chi_\pm}{\partial a}\frac{\partial a}{\partial\rho_2}+\frac{\partial\chi_\pm}{\partial b}\frac{\partial b}{\partial\rho_2}+\frac{\partial\chi_\pm}{\partial c}\frac{\partial c}{\partial\rho_2}=\left[\frac{\partial\chi_\pm}{\partial a}-\frac{\partial\chi_\pm}{\partial c}\right]\frac{\partial a}{\partial\rho_2},$$

where

$$\frac{\partial a}{\partial\rho_2}=S(1-\rho_1\rho_3/\rho_2^2)\ .$$

This is enough to show that $\rho_2^*=\sqrt{\rho_1\rho_3}$ is an extremum.

More explicitly,

$$2\frac{\partial\chi_\pm}{\partial\rho_2}=\frac{1}{a(b^2-4ac)^{1/2}}\{b(b^2-4ac)^{1/2}\pm[2a(a+c)-b^2]\}\frac{\partial a}{\partial\rho_2}\ , \tag{A1}$$

which vanishes only if the quantity in curly brackets vanishes or if $\partial a/\partial\rho_2=0$. One can be shown that the quantity in curly brackets vanishes if and only if $\rho_1=0$ or $\rho_3=0$, as in the case treated in Secs. II. If neither ρ_1 nor ρ_3 vanishes, then the only extremum is at $\rho_2=\rho_2^*=\sqrt{\rho_1\rho_3}$. The nature of this extremum is determined from the second derivative

$$2\frac{\partial^2\chi_\pm}{\partial\rho_2^2}=\frac{1}{a(b^2-4ac)^{1/2}}\{b(b^2-4ac)^{1/2}\pm[2a(a+c)-b^2]\}\frac{\partial^2 a}{\partial\rho_2^2} \tag{A2}$$

at $\partial a/\partial\rho_2=0$. The sign of $\partial^2\chi_\pm/\partial\rho_2^2$ is determined by the sign of the quantity in brackets since a, $(b^2-4ac)^{1/2}$, and $\partial^2 a/\partial\rho_2^2$ are all positive. The proof then consists in showing that

$$b(b^2-4ac)^{1/2}+2a(a+c)-b^2>0 \tag{A3}$$

and

$$b(b^2-4ac)^{1/2}-2a(a+c)+b^2<0\ , \tag{A4}$$

which imply that $\rho_2=\sqrt{\rho_1\rho_3}$ is a minimum for χ_+ and a maximum for χ_-, as indicated in Fig. 2.

The first step in proving the inequalitities (A3) and (A4) is to show that

$$2a(a+c)-b^2>0\ , \tag{A5}$$

which follows, after some algebra, from the inequality $1-S+ST>0$. Inequality (A3) follows trivially from (A5) if $b>0$. If $b<0$, some algebra is needed, but eventually it follows from $\rho_1>0$. Similarly, (A4) follows trivially from (A5) if $b<0$. If $b>0$, it follows from $\rho_3>0$.

APPENDIX B

In this appendix we outline the proof of the inversion and fixed-free theorems. The methods that we present are not unique and, in fact, there are several other ways of proving the same theorems.

The characteristic equation, a polynomial of degree $N-1$, can be obtained either by elimination of the δ_i, or by solving $\det|M-\lambda I|=0$, where $\lambda=gk/\gamma^2=1/\chi$ (not to be confused with wavelength). Our proof of the inversion theorem consists in showing that all the coefficients $a_{N-1},a_{N-2},\ldots,a_1,a_0$ of the characteristic equation [Eq. (20)]

$$a_{N-1}\chi^{N-1}+a_{N-2}\chi^{N-2}+\cdots+a_1\chi+a_0=0 \tag{B1}$$

are invariant under inversion. This implies that the eigenvalues of the inverted profile satisfy the same characteristic equation as the original profile, and therefore $\{\gamma^2\}=\{\gamma^2\}_{\text{inverted}}$.

Let us obtain (B1) by elimination. Define

$$\tilde{\rho}_i=\frac{\rho_i S_i-(1+S_iT_i)\left[(\rho_i-\rho_{i-1})\frac{1}{\chi}-\tilde{\rho}_{i-1}\right]}{1+\frac{S_i}{T_i}-\frac{S_i}{\rho_i}\left[(\rho_i-\rho_{i-1})\frac{1}{\chi}-\tilde{\rho}_{i-1}\right]} \tag{B2}$$

for $i=2,3,\ldots,N-1$, with $\tilde{\rho}_1=\rho_1$. The characteristic equation then reads $\tilde{\rho}_N=\rho_N$, and Eq. (B1) is obtained by expanding this equation. This is an iterative method in which Eq. (B2) is used $N-2$ times until we reach $\tilde{\rho}_1=\rho_1$.

Let us illustrate with $N=5$. The extension to arbitrary N is straightforward but the expressions get too long. Unfortunately, no physical insight is obtained by doing these calculations.

The last of the equations in Eq. (19) reads

$$\rho_5=(\rho_{54})\frac{1}{\chi}-\tilde{\rho}_4\ , \tag{B3}$$

where we have defined $\rho_{ij}\equiv\rho_i-\rho_j$, and used the fact that an alternative definition of $\tilde{\rho}_i$ is

$$\tilde{\rho}_i=\rho_i\left[T_i-\frac{\delta_i}{(1-\delta_i)S_i}\right]\ . \tag{B4}$$

Using Eq. (B2) three times, substitute for $\tilde{\rho}_4$ in terms of $\tilde{\rho}_3$; in the resulting expression, substitute for $\tilde{\rho}_3$ in terms of $\tilde{\rho}_2$ and, finally, again using (B2), substitute for $\tilde{\rho}_2$ in terms of $\tilde{\rho}_1=\rho_1$. We now have an equation in which only the known quantities ρ_i and t_i appear:

$$\rho_5=\rho_{54}/\chi-\frac{\rho_4S_4-(1+S_4T_4)\left[\rho_{43}/\chi-\dfrac{\rho_3S_3-(1+S_3T_3)\left[\rho_{32}/\chi-\dfrac{\rho_2S_2-(1+S_2T_2)(\rho_{21}/\chi-\rho_1)}{1+S_2T_2-\dfrac{S_2}{\rho_2}(\rho_{21}/\chi-\rho_1)}\right]}{1+S_3T_3-\dfrac{S_3}{\rho_3}\left[\rho_{32}/\chi-\dfrac{\rho_2S_2-(1+S_2T_2)(\rho_{21}/\chi-\rho_1)}{1+S_2T_2-\dfrac{S_2}{\rho_2}(\rho_{21}/\chi-\rho_1)}\right]}\right]}{1+S_4T_4-\dfrac{S_4}{\rho_4}\left[\rho_{43}/\chi-\dfrac{\rho_3S_3-(1+S_3T_3)\left[\rho_{32}/\chi-\dfrac{\rho_2S_2-(1+S_2T_2)(\rho_{21}/\chi-\rho_1)}{1+S_2T_2-\dfrac{S_2}{\rho_2}(\rho_{21}/\chi-\rho_1)}\right]}{1+S_3T_3-\dfrac{S_3}{\rho_3}\left[\rho_{32}/\chi-\dfrac{\rho_2S_2-(1+S_2T_2)(\rho_{21}/\chi-\rho_1)}{1+S_2T_2-\dfrac{S_2}{\rho_2}(\rho_{21}/\chi-\rho_1)}\right]}\right]} \tag{B5}$$

After some algebra, we obtain the characteristic equation

$$a_4\chi^4+a_3\chi^3+a_2\chi^2+a_1\chi+a_0=0\ ,$$

where

$$a_0=\frac{S_2S_3S_4}{\rho_2\rho_3\rho_4}\rho_{54}\rho_{43}\rho_{32}\rho_{21}\ ,$$

$$-a_1=(1+S_4T_4)\frac{S_2S_3}{\rho_2\rho_3}\rho_{53}\rho_{32}\rho_{21}+(1+S_2T_2)\frac{S_3S_4}{\rho_3\rho_4}\rho_{54}\rho_{43}\rho_{31}+(1+S_3T_3)\frac{S_2S_4}{\rho_2\rho_4}\rho_{54}\rho_{42}\rho_{21}$$
$$+\frac{S_2S_3S_4}{\rho_3}\rho_{43}\rho_{32}(\rho_5/\rho_4-\rho_1/\rho_2)\ ,$$

$$a_2=(1+S_4T_4)(1+S_3T_3)\frac{S_2}{\rho_2}\rho_{52}\rho_{21}+(1+S_3T_3)(1+S_2T_2)\frac{S_4}{\rho_4}\rho_{54}\rho_{41}+(1+S_4T_4)(1+S_2T_2)\frac{S_3}{\rho_3}\rho_{53}\rho_{31}$$
$$+(1+S_4T_4)S_2S_3\rho_{32}(\rho_5/\rho_3-\rho_1/\rho_2)+(1+S_2T_2)S_3S_4\rho_{43}(\rho_5/\rho_4-\rho_1/\rho_3)$$
$$+(1+S_3T_3)S_2S_4\rho_{42}(\rho_5/\rho_4-\rho_1/\rho_2)+S_2S_3S_4\left[\frac{\rho_{21}}{\rho_2}\left[\frac{\rho_3}{\rho_4}\rho_{54}+\frac{\rho_4}{\rho_3}\rho_{32}\right]+\frac{\rho_{43}}{\rho_3\rho_4}\left[\rho_2\rho_{54}+\frac{\rho_1\rho_5}{\rho_2}\rho_{32}\right]\right]\ , \tag{B6}$$

$$-a_3=(1+S_4T_4)(1+S_3T_3)(1+S_2T_2)\rho_{51}+(1+S_4T_4)(1+S_3T_3)S_2\rho_{51}+(1+S_3T_3)(1+S_2T_2)S_4\rho_{51}$$
$$+(1+S_2T_2)(1+S_4T_4)S_3\rho_{51}+(1+S_4T_4)S_2S_3\left[\frac{\rho_5}{\rho_3}\rho_{21}+\frac{\rho_1}{\rho_2}\rho_{53}+\rho_{32}\right]$$
$$+(1+S_2T_2)S_3S_4\left[\frac{\rho_1}{\rho_3}\rho_{54}+\frac{\rho_5}{\rho_4}\rho_{31}+\rho_{43}\right]$$
$$+(1+S_3T_3)S_2S_4\left[\frac{\rho_5}{\rho_4}\rho_{21}+\frac{\rho_1}{\rho_2}\rho_{54}+\rho_{42}\right]+S_2S_3S_4\left[\frac{\rho_1}{\rho_2}\rho_{43}+\frac{\rho_5}{\rho_4}\rho_{32}+\rho_5\rho_2/\rho_3-\rho_1\rho_4/\rho_3\right],$$

$$a_4=(1+S_4T_4)(1+S_3T_3)(1+S_2T_2)(\rho_5+\rho_1)+\rho_1\rho_5(1+S_3T_3)\left[(1+S_4T_4)\frac{S_2}{\rho_2}+(1+S_2T_2)\frac{S_4}{\rho_4}\right]$$
$$+(1+S_3T_3)[(1+S_4T_4)\rho_2S_2+(1+S_2T_2)\rho_4S_4]+(1+S_4T_4)(1+S_2T_2)S_3(\rho_3+\rho_1\rho_5/\rho_3)$$
$$+(1+S_2T_2)S_3S_4(\rho_1\rho_4/\rho_3+\rho_5\rho_3/\rho_4)+(1+S_4T_4)S_2S_3(\rho_3\rho_1/\rho_2+\rho_5\rho_2/\rho_3)$$
$$+(1+S_3T_3)S_2S_4(\rho_1\rho_4/\rho_2+\rho_5\rho_2/\rho_4)+S_2S_3S_4(\rho_2\rho_4/\rho_3+\rho_1\rho_5\rho_3/\rho_2\rho_4)\ .$$

As a check we note that, by letting any two thicknesses $\to 0$, we obtain the quadratic Eq. (7) for the case $N=3$.

It is straightforward to show that each of a_0, a_1, a_2, a_3, and a_4 is invariant under $\rho_1\to\rho_1$, $\rho_2\to\rho_1\rho_5/\rho_4$, $\rho_3\to\rho_1\rho_5/\rho_3$, $\rho_4\to\rho_1\rho_5/\rho_2$, $\rho_5\to\rho_5$, accompanied by $t_2\to t_4$, $t_3\to t_3$. Hence, the inverted profile satisfies the same characteristic equation (B1) and therefore has the same roots. This completes the proof of the inversion theorem for the case $N=5$. Extension to arbitrary N will not be given here. We will report later if we find a more "elegant" proof.

We now turn to the fixed-free theorem, and first show that $\gamma^2=\pm gk$ are always two possible modes for a density profile between two free boundaries. Note that the boundary conditions read

$$DW+\frac{gk^2}{\gamma^2}W=0\ , \tag{B7}$$

which is obtained from Eq. (3) by setting $\rho_N=\rho_1=0$. Note that the *same* condition is obtained if $W(y)$ *and* $DW(y)$ are continuous across an interface. It follows that the two solutions, $W(y)\sim e^{+ky}$ and $W(y)\sim e^{-ky}$ throughout the whole fluid region,

$$0\le y\le t_{\rm tot}=\sum_{i=2}^{N-1}t_i\ ,$$

satisfy all the boundary conditions if $\gamma^2=-gk$ and $\gamma^2=+gk$, respectively. That this is true for an arbitrary profile, continuous or stepwise, is clear from Eq. (2) also.

When only one boundary is free and the other is not fixed we again have one of the modes $\gamma^2=+gk$ or $-gk$ depending on whether the free boundary is unstable or stable, respectively. If one boundary is free and the other is fixed then, in general, neither one of these two modes are present unless λ is much less than the distance between the two boundaries.

The second part of the fixed-free theorem states that, if the density profile is invariant under inversion, then

$$\{\gamma^2\}_{\rm free}=\{\gamma^2\}_{\rm fixed}\cup\{gk,-gk\}\ ,$$

where $\{\gamma^2\}_{\rm free,fixed}$ refer to the modes of the same profile $\rho_2,\rho_3,\ldots,\rho_{N-1},t_2,t_3,\ldots,t_{N-1}$, between two free or two fixed boundaries. This theorem appears to be an "if and only if" statement, but we have not attempted to prove the "only if" part, which is obviously harder, and we leave it as a conjecture supported only by numerical experience.

Our proof for the "if" part consists in showing that the characteristic equation for the free case reduces to that of the fixed case after we factor out the two modes $\chi=+1$ and $\chi=-1$. We choose to calculate the coefficient a_i the same way as before, setting $\rho_1=\rho_N=0$ for the free case and $\delta_2=\infty,\delta_{N-1}=1$ for the fixed case, when the equation becomes only of order $N-3$. Let

$$a_{N-1}^{\rm free}\chi^{N-1}+a_{N-2}^{\rm free}\chi^{N-2}+\cdots+a_1^{\rm free}\chi+a_0^{\rm free}=0 \tag{B8}$$

and

$$a_{N-3}^{\text{fix}}\chi^{N-3}+a_{N-4}^{\text{fix}}\chi^{N-4}+\cdots+a_1^{\text{fix}}\chi+a_0^{\text{fix}}=0 \tag{B9}$$

be the characteristic equations for the free and fixed cases, respectively. One way to prove the fixed-free theorem is to show that, by multiplying Eq. (B9) by χ^2-1, we get Eq. (B8) if the profile is inversion invariant, i.e., if it does not change under $\rho_i\to 1/\rho_{N+1-i}$ and $t_i\to t_{N+1-i}$, $i=2,\ldots,N-1$. Equating the coefficients of equal powers of χ in this way, the problem is reduced to showing that[11]

$$a_{N-i-2}^{\text{fix}}-a_{N-i}^{\text{fix}}=a_{N-i}^{\text{free}}\ ,\quad i=1,\ldots,N\ . \tag{B10}$$

It must be remembered that $a_l^{\text{fix}}=0$ if $l<0$ or if $l>N-3$. Of course, not all of the N equations in (B10) are independent; they incorporate the fact that $\chi=\pm 1$ are solutions to Eq. (B8) which we have already shown to be true and, therefore,

$$\sum_{i=\text{even}} a_i^{\text{free}}=0\ , \tag{B11}$$

$$\sum_{i=\text{odd}} a_i^{\text{free}}=0\ . \tag{B12}$$

These two constraints are valid for any density profile, while Eqs. (B10), seen as $N-2$ nontrivial relations, are valid only if the profile is invariant under inversion.

Let us illustrate with the case $N=5$. The coefficients a_i^{free} are

$$\begin{aligned}
a_0^{\text{free}}&=-S_2S_3S_4\rho_{43}\rho_{32}/\rho_3\ ,\\
a_1^{\text{free}}&=(1+S_4T_4)S_2S_3\rho_{32}+(1+S_2T_2)S_3S_4\rho_{43}+(1+S_3T_3)S_2S_4\rho_{42}\ ,\\
a_2^{\text{free}}&=-(1+S_4T_4)(1+S_3T_3)S_2\rho_2-(1+S_4T_4)(1+S_2T_2)S_3\rho_3-(1+S_3T_3)(1+S_2T_2)S_4\rho_4\\
&\quad -S_2S_3S_4(\rho_3+2\rho_2\rho_4/\rho_3-\rho_4-\rho_2)\ ,\\
a_3^{\text{free}}&=-(1+S_4T_4)S_2S_3\rho_{32}-(1+S_2T_2)S_3S_4\rho_{43}-(1+S_3T_3)S_2S_4\rho_{42}\ ,\\
a_4^{\text{free}}&=(1+S_4T_4)(1+S_3T_3)S_2\rho_2+(1+S_3T_3)(1+S_2T_2)S_4\rho_4+(1+S_4T_4)(1+S_2T_2)S_3\rho_3\\
&\quad +S_2S_3S_4\rho_2\rho_4/\rho_3\ ,
\end{aligned} \tag{B13}$$

$$\begin{aligned}
a_0^{\text{fix}}&=S_2S_3S_4\rho_{43}\rho_{32}/\rho_3\ ,\\
a_1^{\text{fix}}&=-(1+S_4T_4)S_2S_3\rho_4\rho_{32}/\rho_3-(1+S_3T_3)S_2S_4\rho_{42}-(1+S_2T_2)S_3S_4\rho_{43}\rho_2/\rho_3\ ,\\
a_2^{\text{fix}}&=S_2S_3S_4\rho_3+(1+S_4T_4)(1+S_2T_2)S_3\rho_4\rho_2/\rho_3+(1+S_4T_4)(1+S_3T_3)S_2\rho_4\\
&\quad +(1+S_3T_3)(1+S_2T_2)S_4\rho_2\ .
\end{aligned} \tag{B14}$$

Note that $a_1^{\text{free}}+a_3^{\text{free}}=0$ and $a_0^{\text{free}}+a_2^{\text{free}}+a_4^{\text{free}}=0$. The five relations from Eq. (B.10) are

$$\begin{aligned}
&a_2^{\text{fix}}=a_4^{\text{free}}\ ,\quad a_1^{\text{fix}}=a_3^{\text{free}}\ ,\\
&a_0^{\text{fix}}-a_2^{\text{fix}}=a_2^{\text{free}}\ ,\quad -a_1^{\text{fix}}=a_1^{\text{free}}\ ,\\
&-a_0^{\text{fix}}=a_0^{\text{free}}\ .
\end{aligned} \tag{B15}$$

One can easily check that these relations are satisfied if the profile if invariant under inversion, which in this case means $t_2=t_4$, t_3 arbitrary, and $\rho_3=\rho_4\rho_2/\rho_3$, ρ_2 and ρ_4 arbitrary.

In each case, we have tried to formulate our proof in such a way that extension to arbitrary N is straightforward (albeit nontrivial). We have chosen to work with the coefficients a_i in the characteristic equation. Alternatively, one may study the properties of the matrix M from which the characteristic equation can also be derived. For example, the inversion theorem can also be proved by showing that there exists a nonsingular matrix A such that $M_{\text{inverted}}=AMA^{-1}$. Clearly, $\det|M-\lambda I|=0$ is left invariant under this transformation. The existence of A, however, is not any easier to prove than the invariance of the coefficients in the characteristic equation, although this alternative approach might help our intuitive understanding of inversion symmetry.

We repeat that both theorems are valid for arbitrary wavelengths $2\pi/k$ of perturbations. The proofs are trivial for very short or very long wavelengths.

Finally, we state a corollary to the inversion

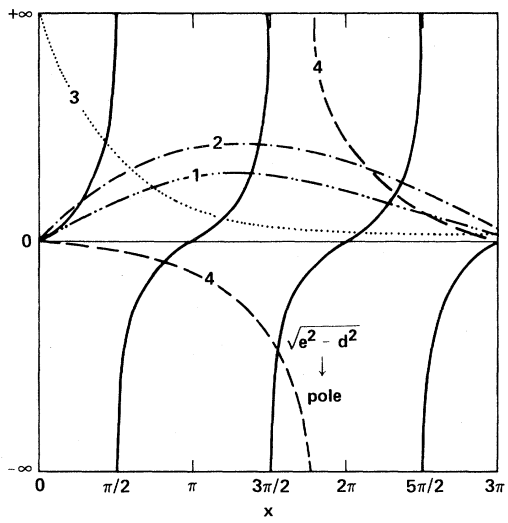

FIG. 7. Intersections of the continuous curves $y=\tan(x)$ with the broken curves $y=2ex/x^2+d^2-e^2$ determine the values of x in Eq. (33). Case (1) is for $e\leq -1+(1+d^2)^{1/2}$; case (2) is for $-1+(1+d^2)^{1/2}<e<d$; case (3) is for $e=d$; and case (4) is for $e>d$. Here $e=kt$ and $d=\beta t/2$. Density profile is exponential, $\rho=\rho_0 e^{\beta y}$, with $\rho=\rho_0$ for $y\leq 0$ and $\rho=\rho_0 e^{\beta t}=\rho_t$ for $y\geq t$ [Fig. 5(e)].

theorem which clarifies the relationship between these two theorems: The spectrum of a density profile between two free boundaries is identical to the spectrum of the inverted profile between two fixed boundaries, except for the two modes $\gamma^2=\pm gk$ which are present in the free case but not in the fixed case.

The proof is similar to the proof of the fixed-free theorem which can be viewed as a special case of this corollary.

APPENDIX C

For an exponential profile $\rho(y)=\rho_0 e^{\beta y}$, $0\leq y\leq t$, the parameter x determines the growth mode γ through Eq. (33). Except for the case of two fixed or two free boundaries, x is found by (numerically) solving a transcendental equation. Since only x^2 enters in Eq. (33), we need to consider only positive values of x or of z where $x=iz$. We will use case E as an illustration in which case x is found from Eq. (52),

$$\tan(x)=\frac{2xe}{x^2+d^2-e^2}\ . \tag{C1}$$

We will also assume that β, and therefore d, is positive.

Let us first consider the imaginary solutions of (C1) since these are few in number. Setting $x=iz$, Eq. (C1) becomes

$$\tanh(z)=\frac{2ze}{d^2-e^2-z^2}\ . \tag{C2}$$

There is only one solution which occurs if $d>e$ and $e<\frac{1}{2}(d^2-e^2)$ [case (1) below].

The situation is different for real x. There are always an infinite number of solutions, the large x solutions being approximately given by $m\pi$, where m is a (large) integer. However, the large x values are not interesting since they give only the slowly growing modes. The faster growing modes have small values of x and we can find four possibilities.

Case (1). $e\leq -1+(1+d^2)^{1/2}$. The smallest value of x is between π and $3\pi/2$.

Case (2). $-1+(1+d^2)^{1/2}<e<d$. The smallest value of x is less than $\pi/2$.

Case (3). $e=d$. Then $x_{\min}<\pi/2$ again.

Case (4). $e>d$. Then $\pi/2<x_{\min}<\pi$. Note that the right-hand side of Eq. (C1) has a pole in this case. If the pole occurs before $\pi/2$, i.e., $(e^2-d^2)^{1/2}<\pi/2$, then $x_{\min}<\pi/2$.

In Fig. 7, we show graphically the solutions to Eqs. (C1) for each of the above four cases. The growth modes $\gamma/\sqrt{g}$ quoted under continuous in Table II were calculated numerically by finding the intersection points of the curves in this figure.

[1]Lord Rayleigh, *Theory of Sound*, 2nd ed. (Dover, New York, 1894), Vol. 2; G. I. Taylor, Proc. R. Soc. London Ser. A 201, 192 (1950).

[2]J. D. Lindl and W. C. Mead, Phys. Rev. Lett. 34, 1273 (1975); J. Nuckolls, J. Lindl, W. Mead, A. Thiessen, L. Wood, and G. Zimmerman, University of California Report No. UCRL-75538 (unpublished).

[3]R. E. Kidder, Nucl. Fusion 16, 3 (1976); D. L. Book and I. B. Bernstein, J. Plasma Phys. 23, 521 (1980).

[4]S. E. Bodner, Phys. Rev. Lett. 33, 761 (1974).

[5]R. L. McCrory, L. Montierth, R. L. Morse, and C. P. Verdon, Phys. Rev. Lett. 46, 336 (1981).

[6]J. D. Lindl, R. O. Bangerter, J. H. Nuckolls, W. C. Mead, and J. J. Thomson, University of California Report No. UCRL-78470 (unpublished); R. Lelevier, G. J. Lasher, and F. Bjorklund, University of California Report No. UCRL-4459 (unpublished).

[7]K. O. Mikaelian, Phys. Rev. Lett. 48, 1365 (1982).

[8]S. Chandrasekhar, *Hydrodynamic and Hydromagnetic Stability* (Oxford University Press, London, 1968).

[9]Since an overall scale for ρ is immaterial, inversion can be defined as $\rho_i \rightarrow 1/\rho_{N+1-i}$ followed by interchange of thicknesses.

[10]Only the eigenvalues γ remain invariant under the inversion of the profile; the associated eigenstates $W^{\gamma}(y)$ are different.

[11]The RHS of Eq. (B10) can be multiplied by an arbitrary constant since the roots of a polynomial equation are not changed if all the coefficients are multiplied by the same constant. Similarly for the inversion theorem all that is needed is to show that $(a_i)_{\text{inverted}} = \text{constant} \times (a_i)_{\text{original}}$.